Statistically background-free, phase-preserving parametric up-conversion with faint light

Y.-H. Cheng,[1,2] **Tim Thomay,**[1,2] **Glenn S. Solomon,**[1,2]
Alan L. Migdall,[1,2] **and Sergey V. Polyakov**[1,*]

[1]*National Institute of Standards and Technology, Gaithersburg, Maryland 20899, USA*
[2]*Joint Quantum Institute, National Institute of Standards and Technology, and University of Maryland, College Park, Maryland 20742, USA*

[*]*spoly@nist.gov*

Abstract: We demonstrate up-conversion with no statistically significant background photons and a dynamic range of 15 decades. Near-infrared 920 nm photons were converted into the visible at 577 nm using periodically poled lithium niobate waveguides pumped by a 1550 nm laser. In addition to achieving statistically noiseless frequency up-conversion, we report a high degree of phase preservation (with fringe visibilities ≥ 0.97) at the single-photon level using an up-converting Mach-Zehnder interferometer. This background-free process opens a path to single-photon detection with no intrinsic dark count. Combined with a demonstrated photon-number preserving property of an up-converter, this work demonstrates the feasibility of noiseless frequency up-conversion of entangled photon pairs.

OCIS codes: (270.5585) Quantum information and processing; (130.7405) Wavelength conversion devices; (270.1670) Coherent optical effects; (270.5565) Quantum communications; (190.4223) Nonlinear wave mixing.

References and links

1. B. Julsgaard, J. Sherson, J. I. Cirac, J. Fiurasek, and E. S. Polzik, "Experimental demonstration of quantum memory for light," Nature **432**, 482–486 (2004).
2. R. Blatt and D. Wineland, "Entangled states of trapped atomic ions," Nature **453**, 1008–1015 (2008).
3. K. De Greve, L. Yu, P. L. McMahon, J. S. Pelc, C. M. Natarajan, N. Y. Kim, E. Abe, S. Maier, C. Schneider, M. Kamp, S. Hofling, R. H. Hadfield, A. Forchel, M. M. Fejer, and Y. Yamamoto, "Quantum-dot spin-photon entanglement via frequency downconversion to telecom wavelength," Nature **491**, 421–425 (2012).
4. W. B. Gao, P. Fallahi, E. Togan, J. Miguel-Sanchez, and A. Imamoglu, "Observation of entanglement between a quantum dot spin and a single photon," Nature **491**, 426–430 (2012).
5. P. Kumar, "Quantum frequency conversion," Opt. Lett. **15**, 1476 (1990).
6. R. Ikuta, T. Kobayashi, H. Kato, S. Miki, T. Yamashita, H. Terai, M. Fujiwara, T. Yamamoto, M. Sasaki, Z. Wang, M. Koashi, and N. Imoto, "Observation of two output light pulses from a partial wavelength converter preserving phase of an input light at a single-photon level," Opt. Express **21**, 27865–27872 (2013).
7. H. Takesue, "Single-photon frequency down-conversion experiment," Phys. Rev. A **82**, 013833 (2010).
8. R. Ikuta, T. Kobayashi, H. Kato, S. Miki, T. Yamashita, H. Terai, M. Fujiwara, T. Yamamoto, M. Koashi, M. Sasaki, Z. Wang, and N. Imoto, "Nonclassical two-photon interference between independent telecommunication light pulses converted by difference-frequency generation," Phys. Rev. A **88**, 042317 (2013).
9. S. Zaske, A. Lenhard, C. A. Keßler, J. Kettler, C. Hepp, C. Arend, R. Albrecht, W.-M. Schulz, M. Jetter, P. Michler, and C. Becher, "Visible-to-telecom quantum frequency conversion of light from a single quantum emitter," Phys. Rev. Lett. **109**, 147404 (2012).
10. R. Ikuta, Y. Kusaka, T. Kitano, H. Kato, T. Yamamoto, M. Koashi, and N. Imoto, "Wide-band quantum interface for visible-to-telecommunication wavelength conversion," Nat. Commun. **2**, 1544 (2011).

#241394 Received 19 May 2015; revised 27 Jun 2015; accepted 29 Jun 2015; published 9 Jul 2015

11. S. Ates, I. Agha, A. Gulinatti, I. Rech, M. T. Rakher, A. Badolato, and K. Srinivasan, "Two-photon interference using background-free quantum frequency conversion of single photons emitted by an InAs quantum dot," Phys. Rev. Lett. **109**, 147405 (2012).
12. A. P. Vandevender and P. Kwiat, "High efficiency single photon detection via frequency up-conversion," J. Mod. Optic. **51**, 1433–1445 (2004).
13. A. P. Vandevender and P. Kwiat, "Quantum transduction via frequency upconversion," J. Opt. Soc. Am. B **24**, 295–299 (2007).
14. D. Ceus, L. Delage, L. Grossard, F. Reynaud, H. Herrmann, and W. Sohler, "Contrast and phase closure acquisitions in photon counting regime using a frequency upconversion interferometer for high angular resolution imaging," Mon. Not. R. Astron. Soc. **430**, 1529–1537 (2013).
15. J.-T. Gomes, L. Delage, R. Baudoin, L. Grossard, L. Bouyeron, D. Ceus, F. Reynaud, H. Herrmann, and W. Sohler, "Laboratory demonstration of spatial-coherence analysis of a blackbody through an up-conversion interferometer," Phys. Rev. Lett. **112**, 143904 (2014).
16. P. S. Kuo, J. S. Pelc, O. Slattery, Y.-S. Kim, M. M. Fejer, and X. Tang, "Reducing noise in single-photon-level frequency conversion," Opt. Lett. **38**, 1310 (2013).
17. Certain commercial equipment, instruments, or materials are identified in this paper to foster understanding. Such identification does not imply recommendation or endorsement by the National Institute of Standards and Technology, nor does it imply that the materials or equipment identified are necessarily the best available for the purpose.
18. S. V. Polyakov, A. Muller, E. B. Flagg, A. Ling, N. Borjemscaia, E. Van Keuren, A. Migdall, and G. S. Solomon, "Coalescence of single photons emitted by disparate single-photon sources: The example of inas quantum dots and parametric down-conversion sources," Phys. Rev. Lett. **107**, 157402 (2011).
19. *physics.nist.gov/fpga*.
20. C. Langrock, E. Diamanti, R. V. Roussev, Y. Yamamoto, M. M. Fejer, and H. Takesue, "Highly efficient single-photon detection at communication wavelengths by use of upconversion in reverse-proton-exchanged periodically poled $LiNbO_3$ waveguides," Opt. Lett. **30**, 1725–1727 (2005).
21. H. Dong, H. Pan, Y. Li, E. Wu, and H. Zeng, "Efficient single-photon frequency upconversion at 1.06 μm with ultralow background counts," Appl. Phys. Lett. **93**, 071101 (2008).
22. J. S. Pelc, L. Ma, C. R. Phillips, Q. Zhang, C. Langrock, O. Slattery, X. Tang, and M. M. Fejer, "Long-wavelength-pumped upconversion single-photon detector at 1550 nm: performance and noise analysis," Opt. Express **19**, 21445 (2011).
23. J.-T. Gomes, L. Grossard, D. Ceus, S. Vergnole, L. Delage, F. Reynaud, H. Herrmann, and W. Sohler, "Demonstration of a frequency spectral compression effect through an up-conversion interferometer," Opt. Express **21**, 3073–3082 (2013).
24. M. A. Albota, F. N. C. Wong, and J. H. Shapiro, "Polarization-independent frequency conversion for quantum optical communication," J. Opt. Soc. Am. B **23**, 918–924 (2006).

1. Introduction

Scalable processing of quantum information is an important goal that motivates researching novel methods of handling quantum states. In this regard, hybrid quantum systems are particularly important as they can circumvent the limitations of a specific quantum system. This is because a physical system generally offers a narrow optimization range for particular quantum properties. For example, detection of quantum states that have arrived at a processing node as telecom-band photons is often less desirable than that of visible photons, because energy per photon in the telecom-band is considerably lower than in the visible, resulting in reduced detection efficiency and high numbers of false counts (dark counts). Also, such quantum states cannot be directly used in typical quantum storage or processing nodes. They need to be faithfully coupled to a material system, such as an atomic ensemble [1], a trapped ion [2] or a quantum dot (QD) [3, 4], requiring unique matching. Other possible uses include frequency-converting entangled states, where the phase between non-factorable components of the quantum state must be preserved. Parametric frequency up- and down-conversion was proposed for this task [5]. For faithful frequency conversion of a quantum state, single-photon purity and phase information should be faithfully transferred to the up-converted state. Therefore, it is of critical importance to achieve low background rates from the parametric process.

The properties of down-converters have been widely studied [6–10], and a recent demonstration showed that the single-photon purity and indistinguishability are preserved during fre-

#241394 Received 19 May 2015; revised 27 Jun 2015; accepted 29 Jun 2015; published 9 Jul 2015

quency up-conversion with a single QD as a photon source [11]. It was also shown that the degree of coherence of up-converted faint light states does not significantly degrade after an up-conversion [12, 13]. This property can be used to make an interferometer with independent up-conversion in both arms, where at least the fringe visibility of ≈0.90(5) was observed [14, 15]. However, the issue of background photons generated by the up-converting crystals still remains open. In a recent study, signal-to-noise figure was significantly improved using extremely narrow notch filters (with a pass-band full width at half maximum (FWHM) on the order of < 0.1 nm) to significantly limit the broad background due to up-converting the anti-stokes field by the strong pump [16].

Here we report an up-converter that intrinsically has an extremely low rate of background counts (our measurement is consistent with zero to within its accuracy), while maintaining high up-conversion efficiency. In addition, we confirm that the phase of a faint state of light is preserved in the up-conversion process, by up-converting a coherent state and demonstrating no loss of coherence to within the experimental uncertainty. Our up-converters have a dynamic range of 15 orders of magnitude for the input power spanning from a few tens of photons per second to approximately a milliwatt. In addition, this is an enabling step towards background-free photon counting and faithful up-conversion of entangled photon states. Our experimental results expand the range and significantly improve the quality of tools available for faithful frequency manipulation of faint quantum states.

2. Experiment

2.1. Experimental setup

The experiment consists of the two parts. To characterize phase preservation in a parametric frequency mixing process, we employed a Mach-Zehnder interferometer with a frequency converter in each arm, thereby making an interferometer with an output wavelength different from that of the input, Fig. 1, c.f. [14, 15]. The frequency converters were two periodically poled (poling period 9.36 μm), magnesium-oxide doped lithium niobate (MgO:PPLN) $\chi^{(2)}$ 10 mm long crystals with ridge waveguides (with cross section of 3 μm $\times$ 5 μm) manufactured by HC Photonics [17]. The crystals were quasi-phase matched (QPM) for a type-0 sum frequency generation (SFG) process, and can be temperature tuned over a ≈3 nm band around 921 nm, a wavelength chosen for our demonstration because it is typical for InAs QD emission [18]. A laser is used as a source to seed the two up-conversion arms. To measure the background generated by each of the up-converters, the coherent state at 919.5 nm is turned off, all the available pump power at 1550 nm is sent to one of the interferometer's arms while the other arm is blocked. The 1550 nm wavelength was chosen for our continuous wave (CW) pump laser because of the wide availability of laser sources at telecom wavelengths, and because it is very far detuned from the signal wavelength of 919.5 nm. Here we used frequency-stabilized, CW diode lasers as pump and signal.

Both the signal and pump beams were combined on a dichroic mirror (DM). Then, they were split into two channels with a polarizing beam splitter (PBS). The power splitting ratio was controlled with half-wave plates before the DM. After splitting at the PBS, the beams were each up-converted to 577.1 nm. For each channel in our setup, the input beams were focused into the PPLN waveguide through an achromatic objective lens (numerical aperture ≈ 0.25). The waveguide temperatures were maintained at ≈24°C for maximum conversion efficiency. After wavelength conversion, the up-converted yellow light was collimated with an aspheric lens (numerical aperture ≈ 0.5). Then the 919.5 nm signal beam and any background photons generated by the strong pump were removed using a band-pass filter (BPF). The BPF is centered at 572 nm with a bandwidth of 28 nm, with a nominal 0.98 transmittance at 577.1 nm and optical density >7 at 919.5 nm. We employed a mirror on a piezoelectric actuator for

#241394 Received 19 May 2015; revised 27 Jun 2015; accepted 29 Jun 2015; published 9 Jul 2015

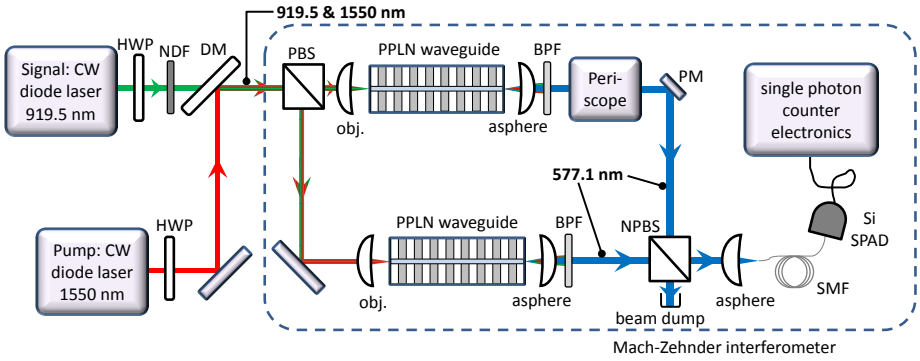

Fig. 1. Mach-Zehnder interferometer up-conversion setup. HWP - half-wave plate, NDF - neutral-density filter, DM - dichroic mirror, PBS - polarizing beam-splitter, obj. - objective lens, asphere - aspheric collimation lens, BPF - band-pass filter, PM - mirror on a piezo-electric actuator, NPBS - non-polarizing beam-splitter, SMF - single-mode fiber, SPAD - single-photon avalanche diode.

sub-wavelength-scale control of the optical path difference between the two arms. To complete the interferometric measurement, we rotated the polarization of one beam so that the two beams had the same polarization when they were recombined on a non-polarizing beam-splitter (NPBS). An output port of the interferometer was coupled into a single-mode fiber (SMF) for detection. The SMF also acts as a spatial filter. We detected the up-converted faint state with a Si single-photon avalanche photodiode (SPAD), and used a field-programmable gate array (FPGA) circuit board [19] to count detection events. Note that the Si SPADs commonly used for photon detection can be operated at room temperature and have a significantly higher detection efficiency for visible light as compared to the wavelengths typical of semiconductor QD emission, a clear benefit of this process.

2.2. *Experimental results*

To characterize the conversion efficiency of our up-converters, we measured the up-converted power as function of pump power. With the measured coupling ratios of the lasers to the two PPLN waveguides, which are 30%/28% and 35%/23% for the wavelengths 919.5/1550 nm, respectively, the internal quantum conversion efficiencies (defined as the number of up-converted photons divided by that of signal photons) of the PPLN waveguides can be estimated, as shown in Fig. 2. The nearly linear trends, particularly at the maximum values ≈20%, show that for the power range investigated in our setup, the efficiency of the QPM SFG process is limited only by available pump laser power.

A high level of background photons, *i.e.* photons that are generated or present at or around the output wavelength when there is no input (at 919.5 nm), is a serious problem in typical up-conversion applications. While significant progress has been made in reducing the background count rate while maintaining record high up-conversion efficiency [16], our goal was to push background levels even lower, even without the use of the volume Bragg gratings used in that previous work.

Here, we examine properties of background photons generated in our setup. To do so, we first used all the available pump power in one up-converting waveguide, and then in the other one. With the BPFs removed, we obtained a photon flux of $\approx 2 \cdot 10^6$ s^{-1} from each of the up-converting crystals. We took spectra of the background for each of the two waveguides with an integration time of 200 s., seen in Fig. 3. It is evident that most of the background counts

#241394 Received 19 May 2015; revised 27 Jun 2015; accepted 29 Jun 2015; published 9 Jul 2015

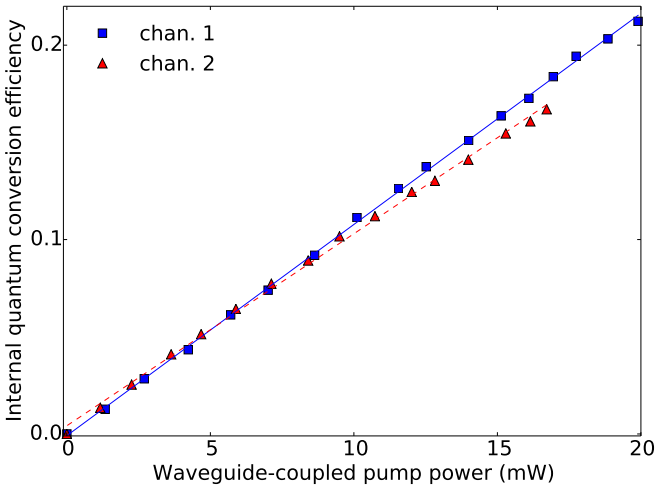

Fig. 2. Internal quantum conversion efficiency vs. input pump power in each arm of the interferometer. Squares and triangles are measured values in each channel, while the lines are linear fits.

occur in the vicinity of 775 nm, *i.e.*, the second harmonic of the 1550 nm pump. This light is due to a non-phase-matched second-harmonic generation by the strong pump and is consistent with prior observations [11, 16]. We observed no evidence of spontaneously-generated photons around the target wavelength of the up-conversion (577 nm), refer to the grayed region in Fig. 3. The average of the two spectra in the grayed region is 0.00001(1) a.u., which demonstrates that there is not detectable bias in the spectrum. Thus, the only requirement for our BPF is that it blocks the second harmonic of the pump.

To measure the background due to the strong pump and non-phase-matched cascaded processes associated with it in the vicinity of the up-conversion wavelength, we reinserted the wide BPF, used the pump at its maximum output power (≈70 mW before coupling into a waveguide) with the 919.5 nm laser blocked and measured the background count rate with the Si SPAD for 25 seconds. Then, we blocked the input to the SPAD and measured dark count rates (DCRs), *i.e.*, count rates that are not associated with photoelectronic events, also for 25 seconds. This measurement cycle was repeated 20 times. To infer the background generated in our setup, we assessed background and dark count rates along with the measurement accuracy. The accuracy was assessed using two methods: first, we calculated uncertainty as a standard deviation of the mean for a series of 20 measurements. Then, we calculated uncertainty assuming that the underlying random process is a stationary Poisson process. The two estimations of uncertainty agree. Then, we subtracted the DCRs from the measured background count rates, and accounted for transmittance and detection losses. Our measurement of the background count rates is consistent with zero, to within statistical uncertainties for both waveguides used, see Table 1. The accuracy of our background measurement is limited only by the dark counts of the SPAD used. Thus, our up-converters have an operational dynamic range of input signal photon fluxes (at 919.5 nm) from as few as 20 photons per second to all the way to 10^{16} photons per second, maintaining an output linear with the input. Our background measurements surpass the best results reported to date [16], in both background counts generated by the up-converter and the signal-to-noise benchmark introduced in that work. That signal-to-noise benchmark is a fair way to compare up-converters with different conversion efficiencies, because both background noise and optical losses (including conversion efficiency below unity) diminish its value. For

#241394 Received 19 May 2015; revised 27 Jun 2015; accepted 29 Jun 2015; published 9 Jul 2015

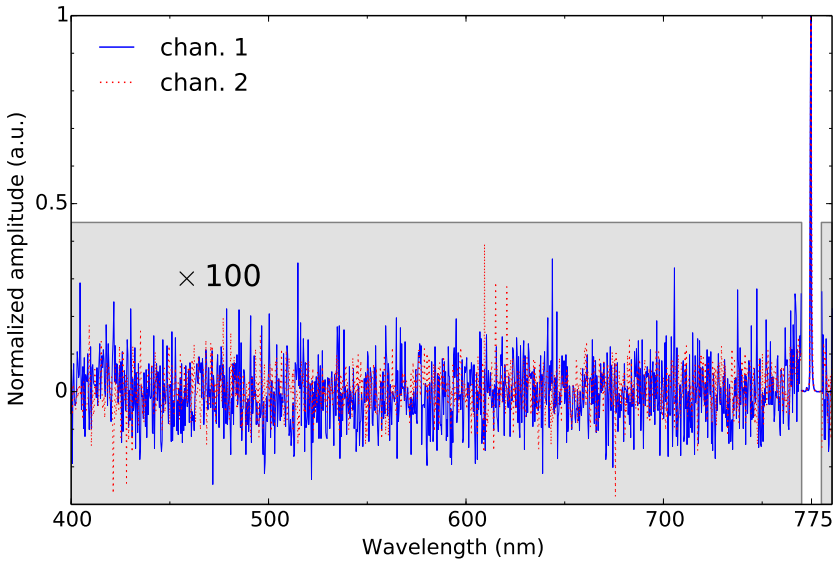

Fig. 3. Background spectra of up-converters. The peak of background *i.e.* at 775 nm is due to second-harmonic generation of the 1550 nm strong pump. The expanded scale regions (grey) show no background at the wavelength range of interest (*i.e.* around 577 nm).

direct comparison, we adopt the convention of [16], where the input signal is set at 4.17×10^5 counts per second, and the loss due to detection efficiency is excluded. We obtain a signal-to-noise figure of ≈5500, higher by an order of magnitude than the highest number observed in Ref. [16] that corresponds to ≈35% conversion efficiency. Here we added *three* standard deviations to the measured background to obtain an upper limit for our background, *i.e.* we used worst-case-scenario data from our setup. Additionally, our bandpass filter is >500x broader than that used in [16]. Had we used a similar narrow notch filter, we estimate our signal-to-noise value would improve further by one order of magnitude.

This background is expected to be very low, for two reasons. First and foremost, a large spectral separation (≈630 nm) of the input faint light (signal) and the strong pump reduces the anti-stokes generation around the signal wavelength to effectively zero [20–22]. This is because the anti-stokes generation rate depends exponentially on spectral separation from the strong pump, and in our case the spectral separation is roughly 4 times larger than that in [16]. Therefore, assuming that background is only due to the anti-stokes process from a strong pump, and that scaling remains exponential, our expected background should be reduced by ≈7 orders of magnitude relative to [16]. Second, a clean, spectrally narrow pump laser source limits the non-phase-matched cascaded processes that could generate noise photons at the target wavelength.

Next we determined fringe visibility in our up-converting Mach-Zehnder interferometer, defined as $\mathscr{V} = (R_{\max} - R_{\min})/(R_{\max} + R_{\min})$, where $R_{\max}$ and $R_{\min}$ are the maximum and minimum count rates, respectively. The laser power at 919.5 nm was attenuated to obtain photon fluxes in the range from $2\cdot10^5$ s^{-1} to $4\cdot10^7$ s^{-1}. High-contrast fringes with visibilities of up to 0.98 were observed, shown in Fig. 4. To obtain $R_{\max}$ and $R_{\min}$, we fitted their extrema with parabolas, and averaged over at least 16 extrema. We use this method rather than fitting sine functions to reduce the effect of the nonlinear behavior of the piezoelectric actuator.

The raw visibility is summarized in Table 2. Notice it drops for lower signal fluxes. To better

#241394 Received 19 May 2015; revised 27 Jun 2015; accepted 29 Jun 2015; published 9 Jul 2015

Table 1. Background count rates at ≈577 nm from sum frequency generating (SFG) waveguides due to strong pump. The generated background is the detected, dark count rate (DCR)-subtracted photon flux, corrected for crystal and optics transmission, coupling, and detection efficiency losses. Stated uncertainties represent one standard deviation statistical uncertainties.

waveguide #	measured background, s^{-1}	measured DCR, s^{-1}	background attributed to SFG, detected by a SPAD, s^{-1}	background generated by a SFG waveguide, s^{-1}
1	82.1(5)	82.5(4)	-0.4(6)	-2(3)
2	86.0(5)	85.7(4)	0.3(6)	1(3)
average	–	–	-0.1(4)	-1(2)

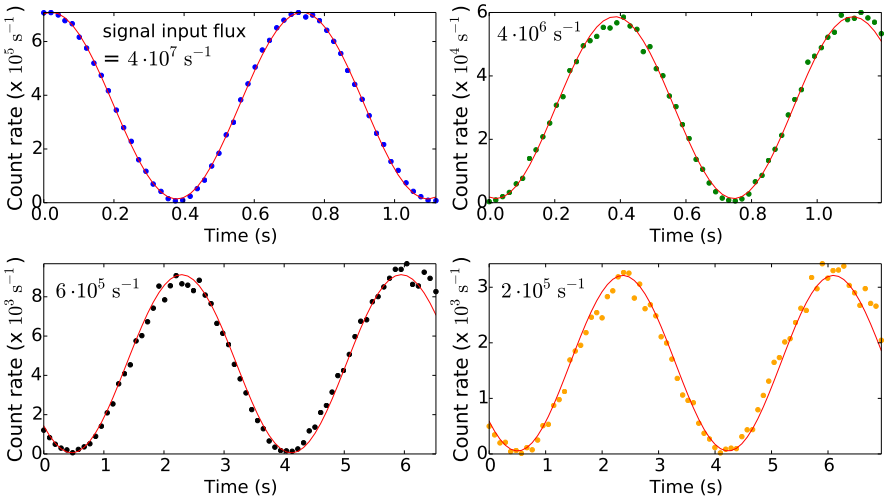

Fig. 4. Experimental demonstration of the interference fringes between the two up-converted beams with faint coherent state input at 919.5 nm at four input light levels. (dots: data; line: sine fit, provided as a guide to the eye)

understand this, we subtracted the independently measured detector DCR from the fringe data. We see that correcting just for the detector DCR restores high visibility at lower input fluxes. Thus, the observed visibility loss is solely due to the detector performance, and not a property of our Mach-Zehnder interferometer. Hence, we have demonstrated that high fringe visibility is independent of the input photon flux, and achieved a significantly higher visibility than the $V \approx 0.90(5)$ achieved in the previous demonstration of interference in a similar configuration [14, 15]. A high degree of phase stability in our interferometer is a very important result for handling photonic qubits and entangled states. A similar visibility was demonstrated in [23], with an input power that is ≈6 orders of magnitude greater than ours. However, observing high visibility fringes with significantly lower input photon fluxes requires an extra test, because, for instance, any background would compromise such a high degree of visibility. Testing of this interferometer with much lower input photon fluxes, as have been done here is important for various applications, such as those in quantum optics. This result may be further improved with active stabilization of the interferometer.

#241394 Received 19 May 2015; revised 27 Jun 2015; accepted 29 Jun 2015; published 9 Jul 2015

Table 2. Observed visibilities for four different 919.5 nm photon fluxes.

methods \ input light flux (s^{-1})	$4{\cdot}10^7$	$4{\cdot}10^6$	$6{\cdot}10^5$	$2{\cdot}10^5$
extrema with local fits	0.98(1)	0.98(1)	0.96(2)	0.93(1)
extrema with local fits and subtraction of DCR	0.98(1)	0.98(1)	0.98(2)	0.97(1)

3. Conclusion

In conclusion, we have experimentally shown that up-conversion in waveguides can be implemented so that it contributes virtually zero background count rate. This is important for many applications, including background and darkcount-free photon counting. Our up-converter arrangement is capable of handling photon fluxes of as few as 20 photons per second and up to 10^{16} photons per second with no adjustments needed. In addition, we demonstrated high fidelity frequency up-conversion (with fringe visibility of $\approx$0.98) important for frequency-shifting of qubits and entangled states. Our result will be particularly useful for up-converting polarization-entangled states while maintaining phase, (c.f. [24]); for example, from polarization-entangled down-converted pairs, or those from a QD biexciton-exciton cascade. The current experimental setup is nearly identical to what would be required for this. Converting our setup for the up-conversion of entangled states requires removing the periscope and replacing the last NPBS before the detection by a PBS to properly recombine the two polarization components of the up-converted state.

Acknowledgments

The authors thank Joffrey Peters for technical assistance with FPGAs. SVP thanks Sofia A. Kostyorkina for encouraging discussions. This work was supported in part by the NSF through Physics Frontier Center at the Joint Quantum Institute.